Observer design for an electrochemical model of lithium ion batteries based on a polytopic approach

Pierre G Blondel, Romain Postoyan, Stéphane Raël, Sébastien Benjamin, Phillippe Desprez

Observer design for an electrochemical model of lithium ion batteries based on a polytopic approach

Pierre G. Blondel [*,**,***,****] **Romain Postoyan** [*,**]
Stéphane Raël [***] **Sébastien Benjamin** [****]
Phillippe Desprez [****]

[*] *Université de Lorraine, CRAN, UMR 7039, Vandoeuvre-les-Nancy,54000 France*
[**] *CNRS, CRAN, UMR 7039,Vandoeuvre-les-Nancy, 54000 France, (e-mails: {pierre.blondel,romain.postoyan}@univ-lorraine.fr)*
[***] *Université de Lorraine, GREEN, (e-mail: stephane.rael@univ-lorraine.fr)*
[****] *SAFT, Direction de la Recherche, Bordeaux, 33000 France, (e-mails: {Sebastien.BENJAMIN,Philippe.DESPREZ}@saftbatteries.com)*

Abstract: Smart battery management systems require reliable state information, which is unavailable through direct measurements. Electrochemical models are relevant in this context as these describe the internal phenomena, which govern the battery. These models can thus be used to design observers and hence to estimate the state variables on-line. We propose an electrochemical model of a lithium ion battery given by a set of ordinary differential equations built from the spatial discretisation of partial differential equations that locally describe mass and charge transport of the lithium. We then design an observer and analyse its stability via a polytopic approach, which relies on the satisfaction of linear matrix inequalities. The latter are shown to be verified for standard model parameters values. Simulation results on the original infinite-dimensional model are presented, which show the good performance of the observer.

Keywords: Control applications, nonlinear models, observers, Lyapunov stability, batteries.

1. INTRODUCTION

Energy storage for embedded systems remains one of the technical challenges of the twenty-first century. Introduced in the early nineties, lithium-ion (Li-ion) batteries have swamped the embedded systems from phones to electric cars. Compared to other electrochemical devices, Li-ion batteries exhibit a high weight power density, a high volumic power density, a low self discharge current and do not suffer from the memory effect. On the other hand, this technology requires a careful management, as recently demonstrated in the media.

One way to improve battery management systems is to estimate the lithium concentrations in different locations in order to improve the knowledge of the State Of Charge (SOC), the state of health or the state of function. This approach requires the development of accurate electrochemical models as well as the design of state observers.

Several techniques are availlable to estimate the SOC. The simplest technique is the Open Circuit Voltage (OCV) versus SOC map. Unfortunately, OCV cannot be measured at any time but only at resting states, i.e. when no current is applied to the battery. Another simple technique, not subject to this limitation, is the Coulomb counting method as in Kong Soon et al. (2009). It consists in counting the electrons that goes in or out of the battery. This is done by integrating the current over the time, which leads to an accumulation of measurement inaccuracies and is therefore non-robust. Coulomb counting is broadly used in the industry but requires sophisticated measurements and readjusting solutions.

Another way to estimate the SOC are observer-based approaches, which can be divided in two categories. The first category relies on Equivalent Circuit Models (ECM), which are simple electrical analogies of the battery dynamics that essentially consist of few coupled resistors and capacitors in series and parallel. The design of these ECM-based techniques is usually easy but the models are simplistic. Hence, a parametrisation is needed, which can either be data-driven see Saha et al. (2009) or done by a bank of Kalman filters as in Plett (2004) or Urbain et al. (2007). The second category relies on electrochemical models, which provide a more faithful description of the battery dynamics but which are usually more difficult to handle. These models describe the dynamics of lithium concentration at different locations of the battery. To know these concentrations allows to deduce the SOC. In this paper, we follow the latter approach as we believe that electrochemical models are a promising step towards the developments of advanced battery management systems. In Doyle et al. (1993), the authors propose a full electro-

chemical model known as pseudo-2D model, which locally describes the electrochemical phenomena through coupled Partial Differential Equations (PDE). Improvement of this work has been done in Smith and Wang (2006) and Prada et al. (2013) but to solve these models is computationally intensive, which make their implementation on embedded devices difficult. A specific reduction of these models is known as Single Particle Model (SPM) see (Di Domenico et al., 2010), where the electrodes are approximated as spherical particles. This type of model, less accurate but computationnally lighter than the previous ones, has been used for the development of various estimation techniques, see the PDE estimator in Moura et al. (2012), the extended Kalman filter in Di Domenico et al. (2010), the unscented Kalman filter in Santhanagopalan and White (2010) or the deterministic finite-dimensional observer in Dey et al. (2015).

In this paper, we aim at designing an observer for an electrochemical model. We first propose a SPM model given by a set of ordinary differential equations (ODE) that represents the lithium diffusion of each electrodes. This model is obtained by spatial discretisation of the partial differential equations governing the diffusion of the lithium and takes the form of an affine dynamical system with a nonlinear output map. It differs from the SPM model considered in Dey et al. (2015), which only describes the diffusion phenomenon in the negative electrode and which deduces the surface concentration of the positive electrode (needed for the output voltage computation) via a transfer function based on the mass conservation of the lithium. We then design an observer for our model. It appears that none of the observer designs for systems with nonlinear output maps we are aware of is applicable to our system, either because the model is not of the right form (Fan and Arcak (2003)), or because the required assumptions are not satisfied (Johansson and Medvedev (2003), Dey et al. (2015)). We therefore propose a new observer. The idea is to interpret the output map as a polytopic term and to use polytopic techniques to design the observer gain, similar to what is done in Zemouche et al. (2008) where nonlinear systems with linear output maps are investigated. The uniform global exponential stability of the origin of the estimation error is established and a $\mathcal{L}_2$-stability property is shown to hold in presence of model disturbance and measurement noises, which is relevant for robustness reasons. These results rely on the satisfaction of matrix inequalities, which are to be verified for standard model parameter values. Compared to (Moura et al. (2012)), we work with finite-dimensional dynamical systems that are easier to implement in practice, which is essential in industrial applications. Contrary to (Di Domenico et al. (2010) or Santhanagopalan and White (2010)), the observer stability is established, which is also crucial for the final application. We have finally implemented the observer on the original infinite-dimensional system and good estimation performances are obtained, even for high currents.

The remainder of the paper is organized as follows. The electrochemical model is described in Section 2. The design of the observer and its analysis are provided in Section 3. In Section 4, we present simulation results on the original infinite-dimensional model. Section 5 concludes the paper.

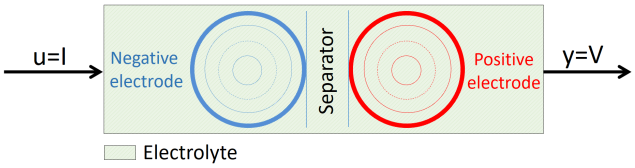

Fig. 1. Battery schematic

The parameters, the symbols, the indexes, the subscripts and the superscripts used throughout the paper are defined in the appendix.

Notations. Let $\mathbb{R} := (-\infty, \infty)$, $\mathbb{R}_{\geq 0} := [0, \infty)$, and $\mathbb{R}_{>0} := (0, \infty)$. We use I_n to denote the identity matrix of size n. For $A \in \mathbb{R}^{N\times M}$, A^T stands for the transpose of A. For $x \in \mathbb{R}^N$ and $y \in \mathbb{R}^M$, (x, y) denotes $(x^T, y^T)^T$. For any symmetric matrix $A \in \mathbb{R}^{N\times N}$, $\lambda_{\min}(A)$ stands for the smallest eigenvalue of A and $\lambda_{\max}(A)$ for the biggest eigenvalue of A. The symbol $*$ in a matrix is for the symmetric term, i.e. $\begin{bmatrix} A & B \\ * & C \end{bmatrix} = \begin{bmatrix} A & B \\ B^T & C \end{bmatrix}$. Let $f : \mathbb{R}^+ \to \mathbb{R}^n$, $\|f\|_{2,[0,t)}$ denotes the $\mathcal{L}_2$ norm of f on the interval $[0, t)$, where $t \in [0, \infty)$, i.e. $\|f\|_{2,[0,t)} = \sqrt{\int_0^t |f(s)|^2 ds}$, when it is well-defined. We write that $f \in \mathcal{L}_2$, when $\|f\|_{2,[0,\infty)} < \infty$. Finally, for $x \in \mathbb{R}^N$, $|x|$ stands for the Euclidean norm of x.

2. ELECTROCHEMICAL MODEL

The electrochemical model describes the solid diffusion of the lithium that occurs in the solid phase of the electrodes. It is derived from a PDE-based model given in Raël and Hinaje (2013) and takes the form of a finite-dimensional nonlinear state-space representation.

We first generally present the system, then we derive the model of the solid diffusion of lithium in the electrodes and finally we give the output of the model. The parameters used in this section are defined in Table A.1 in the appendix.

2.1 Description

A Li-ion battery cell is composed of four components: the negative electrode, the positive electrode, the separator and the electrolyte, see Figure 1. The electrodes are separated by the well-named separator and those three components are immersed in the electrolyte. The electrolyte is a ionic solution that can exchange lithium with the electrodes and provides these electrical insulation. Hence, electrons cannot be exchanged from one electrode to the other within the battery. The potential difference observed between the two electrodes is due to the electrochemical couples located within and between each component. The electrodes are made of porous materials composed of very small, almost-spherical particles. This structure lets the electrolyte penetrate inside the electrode and there is a large contact surface between these.

To simplify the electrochemical model, we assume that the behaviour of a single particle of the average size of the particles in the electrode represents the behaviour of the

whole electrode as, for instance, in Dey et al. (2015), which corresponds to the following assumption.

Assumption 1. Each electrode in the model is composed of a single particle, which is a sphere of the average size of the particles that compose the actual electrode. □

Assumption 1 neglects the thickness of the electrode allowing a significant reduction of the order of the model and leads to a friendly state space form. Again, we will see in Section 3 that although the observer will be designed on a simplified model, good performances are obtained in simulations of an infinite-dimensional model, which does not rely on Assumption 1. We also make the next assumption on the electrolyte.

Assumption 2. The electrolyte is neglected. □

Model simulations with standard set of parameters used in this paper show that the contribution of the electrolyte to the dynamics of the model and to the output voltage is negligible for reasonable currents. Assumption 2 simplifies the model and has a low impact on its accuracy.

Temperature affects various parameters of the battery and is affected by the current and the other states dynamics. In this work, we assume that the temperature is constant. We plan to take it into account in the future.

Assumption 3. Temperature is taken as constant. □

We start by assuming that the model parameters are known and leave the estimation of some of them, like diffusions coefficients, for future work.

Assumption 4. All the parameters of the model are known. □

2.2 Solid diffusion in a particle

In view of Assumptions 1-3, the main physical phenomenon is the lithium diffusion in the electrodes. Lithium diffusions in the negative and in the positive electrode are ruled by the same physical law, only the parametrisation changes from one electrode to the other.

According to Assumption 1, the negative and the positive particles are spheres. The concentration of solid lithium with respect to r, the radial coordinate, is driven by the solid diffusion equation, which is described by the following PDE

$$\frac{\partial c_s(r,t)}{\partial t} = \frac{1}{r^2}\frac{\partial}{\partial r}\left[D_s r^2 \frac{\partial c_s(r,t)}{\partial r}\right], \tag{1}$$

where c_s is the lithium concentration in solid phase, along with two boundaries conditions,

$$\left.\frac{\partial c_s(r)}{\partial r}\right|_{r=0} = 0 \qquad \left.\frac{\partial c_s(r)}{\partial r}\right|_{r=R_s} = K_I^s I, \tag{2}$$

with I the current, $a_s := \dfrac{3\varepsilon_s}{R_s}$ and, under active sign convention, $K_I^{neg} := \dfrac{S_{neg}}{V_{neg}a_{neg}F\mathcal{A}_{cell}d_{neg}}$, $K_I^{pos} := \dfrac{-S_{pos}}{V_{pos}a_{pos}F\mathcal{A}_{cell}d_{pos}}$; we recall that all the subscripts, superscripts and indexes are given in Table A.2 in the appendix. The boundary condition at $r = 0$ means that there are no lithium flux in the center of the sphere for geometrical reasons. The boundary condition in $r = R_s$ means that the flux through the surface of the sphere is proportional to the battery current.

To solve (1) and (2) is intensive in terms of computation, which makes it difficult to implement in an embedded system. We therefore discretize these spatially to obtain a set of ODEs. We consider N_s samples in each particle. The size of each sample is voluntarily not given because any sampling rule can be chosen to discretize the particles. Samples with equivalent radius are chosen in Section 4 to generate numerical values of the electrochemical model but samples with equivalent volume are relevant too.

Let S_n and V_n be the external surface and the volume of the sample $n \in \{1,\dots,N_s\}$, respectively. We spatially discretize equations (1) and (2), for $n \in \{2,\dots,N_s-1\}$,

$$\begin{aligned}\frac{dc_n}{dt} = &\frac{S_{n-1}}{r_n - r_{n-1}}\frac{D_s}{V_n}c_{n-1}\\ &-\left(\frac{S_{n-1}}{r_n - r_{n-1}} + \frac{S_n}{r_{n+1} - r_n}\right)\frac{D_s}{V_n}c_n\\ &+\frac{S_n}{r_{n+1} - r_n}\frac{D_s}{V_n}c_{n+1},\end{aligned} \tag{3}$$

for $n = 1$

$$\frac{dc_1}{dt} = \frac{S_1}{r_2 - r_1}\frac{D_s}{V_1}(-c_1 + c_2), \tag{4}$$

and for $n = N_s$

$$\frac{dc_{N_s}}{dt} = \frac{S_{N_s-1}}{r_{N_s} - r_{N_s-1}}\frac{D_s}{V_{N_s}}(c_{N_s-1} - c_{N_s}) + K_I^s I. \tag{5}$$

The battery does not acquire or leak lithium materials over short time horizons. A mass conservation of the lithium in solid phase equation can therefore be written. Let N_{neg} and N_{pos} be the number of samples the negative and the positive electrode radially discretised, respectively. The quantity of lithium in solid phase is defined as

$$Q := \alpha_{neg}\sum_{i=0}^{N_{neg}} c_i^{neg}V_i^{neg} + \alpha_{pos}\sum_{i=0}^{N_{pos}} c_i^{pos}V_i^{pos}, \tag{6}$$

with $\alpha_{neg} := \dfrac{F}{3600}\dfrac{\varepsilon_{s,neg}\mathcal{A}_{cell}d_{neg}}{V_{s,neg}}$ and $\alpha_{pos} := \dfrac{F}{3600}\times\dfrac{\varepsilon_{s,pos}\mathcal{A}_{cell}d_{pos}}{V_{s,pos}}$. The term Q is expressed in Ah, which explains the scaling term $\dfrac{F}{3600}$ in α_{neg} and α_{pos}.

To reduce the order of the model, we express the concentration of lithium at the center of the negative electrode c_1^{neg} as a linear combination of all the other sampled concentration in solid phase

$$c_1^{neg} = K + \sum_{i=2}^{N_{neg}}\beta_i^{neg}c_i^{N_{neg}} + \sum_{i=1}^{N_{pos}}\beta_i^{pos}c_i^{N_{pos}} \tag{7}$$

with

$$\begin{aligned}K &:= \frac{Q}{\alpha_{neg}V_1^{neg}}\\ \beta_i^{neg} &:= -\frac{V_i^{neg}}{\alpha_{neg}V_1^{neg}} \qquad \beta_i^{pos} := -\frac{\alpha_{pos}V_i^{pos}}{\alpha_{neg}V_1^{neg}}.\end{aligned} \tag{8}$$

This simple reduction appears to be very useful to ensure the satisfaction of the conditions for the stability of the observer in Section 3.

Let $x := (c_2^{neg},\dots,c_{N_{neg}}^{neg},c_1^{pos},\dots,c_{N_{pos}}^{pos}) \in \mathbb{R}^N$ with $N := N_{neg} - 1 + N_{pos}$ be the vector of lithium concentration in

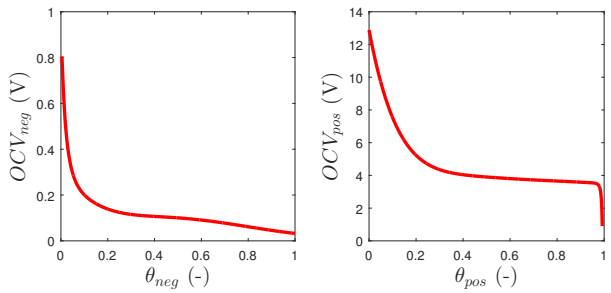

Fig. 2. OCV curves extracted from an empirical formula given by Smith and Wang (2006) with $\theta_{neg} := c_{neg}^{surf}/c_{s,neg}^{max}$ and $\theta_{pos} := c_{pos}^{surf}/c_{s,pos}^{max}$.

each sample of both electrodes and $u \in \mathbb{R}$ be the current I. From (3), (5), (7) and (8), we obtain

$$\dot{x} = Ax + Bu + K, \tag{9}$$

where $A \in \mathbb{R}^{N\times N}$ and $B \in \mathbb{R}^N$ are constant matrices whose expressions follow from (3), (5), (7), and K is a known constant defined in (8); recall that all parameters are known according to Assumption 4.

2.3 Output voltage

As the current is the input and the temperature is taken as constant (see Assumption 3), the output voltage is the only measurable quantity of the battery, i.e. the only output of our model.

The main components of the output voltage are the potential differences between the electrodes and the electrolyte called OCV, which vary with the lithium concentration at the surface between the electrolyte and the electrodes. Hence, in view of Assumption 1, the OCV depends on the lithium concentration at the surface of the sphere c_{N_s}. Figure 2 shows standard OCV curves for Li-ion batteries. Under Assumption 1-3, the output voltage, $y \in \mathbb{R}$, can be obtained from those maps knowing the surface lithium concentration of each particles and the current, leading to

$$y := OCV_{pos}(c_{pos}^{surf}) - OCV_{neg}(c_{neg}^{surf}) + g(u), \tag{10}$$

where $g(u)$ is the current dependent component of the output, whose expression is provided in Appendix B.

3. OBSERVER DESIGN AND ANALYSIS

System (9), (10) belongs to the following class of systems

$$\begin{cases} \dot{x} = Ax + Bu + K + Ew \\ y = h(x) + g(u) + Dz, \end{cases} \tag{11}$$

where h is continuous. In (11), we consider exogenous perturbations $w \in \mathbb{R}^{n_w}$ as well as measurement noise $z \in \mathbb{R}^{n_z}$. Equation (11) is similar to equation (10) in Dey et al. (2015), however the structure of the matrices A, B and K in Section 2 differs due to the fact that we consider both electrodes. As a result, the observer design in Dey et al. (2015) is not applicable here.

We propose the following observer

$$\begin{cases} \dot{\hat{x}} = A\hat{x} + Bu + K + L(y - \hat{y}) \\ \hat{y} = h(\hat{x}) + g(u), \end{cases} \tag{12}$$

where $\hat{x} \in \mathbb{R}^{n_x}$, is the state estimate, $L \in \mathbb{R}^{n_x}$ is the observation matrix gain to be designed with n_x the dimension of the vector x, ($n_x = N$ in Section 2).

Let $e := x - \hat{x}$ denote the estimation error. In view of (11) and (12),

$$\dot{e} = Ae + Ew - L(h(x) - h(\hat{x})) - LDz. \tag{13}$$

We make the following assumption on the output map h.

Assumption 5. For any x, $x' \in \mathbb{R}^{n_x}$ there exist constant matrices $C_1, \dots, C_{2^{n_x}} \in \mathbb{R}^{1\times n_x}$ such that

$$h(x) - h(\hat{x}) = C(x, x')(x - x'), \tag{14}$$

where $C(x,x') = \sum_{i=1}^{2^{n_x}} \lambda_i(x,x')\, C_i$, $\lambda_i(x,x') \in [0,1]$, $\sum_{i=1}^{2^{n_x}} \lambda_i = 1$ and $i \in \{1, \dots, 2^{n_x}\}$. □

Assumption 5 means that the matrix $C(x,x')$ lies in a polytope defined by the vertices C_i, $i \in \{1, \dots, 2^{n_x}\}$. This assumption is verified for instance when h is continuously differentiable and $h(x) = \sum_{i=1}^{n_x} h_i(x_i)$, with $\underline{h_i} \le \dfrac{\partial h_i(x_i)}{\partial x_i} \le \overline{h_i}$ for almost all $x_i \in \mathbb{R}$ with $\underline{h}_i, \overline{h}_i \in \mathbb{R}$. The definitions of the matrices C_i, $i \in \{1, \dots, 2^{n_x}\}$, then follow.

The output given in Section 2.3 satisfies this Assumption 5. Indeed, in practice, the OCVs are given by a set of experimental points. We then construct the h_i's through (linear) interpolation. The maps obtained have bounded derivatives (almost everywhere), though possibly steep ones in view of Figure 2. In our case, the map $h(x) = OCV_{pos}(c_{pos}^{surf}) - OCV_{neg}(c_{neg}^{surf})$ only depends on two states of the system: the surface lithium concentration of the negative and the positive electrode. This leads to a set of C_i's compounded to only 2^2 elements and not 2^{n_x}.

Using Assumption 5, (13) becomes

$$\dot{e} = (A - LC(x,\hat{x}))\, e + Ew - LDz. \tag{15}$$

The idea is to design a common matrix L for each vertex of the polytope defined by the matrices C_i with $i \in \{1, \dots, 2^{n_x}\}$ as in polytopic approaches. We can now state the main stability result.

Theorem 1. Suppose Assumption 5 holds, consider system (15) and let $\mathcal{H}_i := (A - LC_i)^T P + P(A - LC_i)$. If there exist $\varepsilon, \mu_w, \mu_z \in \mathbb{R}_{>0}$ and $P \in \mathbb{R}^{n_x\times n_x}$ symmetric and positive definite such that for $i \in \{1, \dots, 2^{n_x}\}$

$$\begin{pmatrix} \mathcal{H}_i + \varepsilon I_{n_x} & PE & -PLD \\ * & -\mu_w I_{n_w} & 0 \\ * & * & -\mu_z I_{n_z} \end{pmatrix} \le 0, \tag{16}$$

then system (15) is $\mathcal{L}_2$-stable from w and z to e with gain less than or equal to $\sqrt{\frac{\mu_w}{\varepsilon}}$ and $\sqrt{\frac{\mu_z}{\varepsilon}}$, respectively, i.e. there exists $c \ge 0$ such that for any initial condition $e_0 \in \mathbb{R}^{n_x}$, any w,$z \in \mathcal{L}_2$, the corresponding solution e to (15) verifies for any $t \ge 0$

$$\|e\|_{2[0,t)} \le c|e_0| + \sqrt{\frac{\mu_w}{\varepsilon}}\|w\|_{2,[0,t)} + \sqrt{\frac{\mu_z}{\varepsilon}}\|z\|_{2,[0,t)}. \tag{17}$$

Furthermore, when $w = 0$ and $z = 0$, $e = 0$ is uniformly globally exponentially stable (UGES), i.e. there exist γ_1,

$\gamma_2 \in \mathbb{R}_{>0}$, such that for any $e_0 \in \mathbb{R}^{n_x}$, the corresponding solution e to (15) satisfies $|e(t)| \leq \gamma_1 |e_0| e^{-\gamma_2 t}$ for any $t \geq 0$.

□

Proof. Let $e \in \mathbb{R}^{n_x}$, $w \in \mathbb{R}^{n_w}$, $z \in \mathbb{R}^{n_z}$ and $V(e) := e^T P e$ where P comes from Theorem 1. We omit the arguments of λ_i and C in the following. In view of (15),

$$\begin{aligned} &\langle \nabla V(e), (A - LC)\, e + Ew - LDz \rangle \\ &\quad = 2 \sum_{i=1}^{2^{n_x}} \lambda_i \left((A - LC_i)e + Ew - LDz \right)^T Pe, \end{aligned} \tag{18}$$

recall that $\sum_{i=1}^{2^{n_x}} \lambda_i = 1$. We introduce $\chi := (e, w, z)$ and we deduce from (18)

$$\begin{aligned} &\langle \nabla V(e), (A - LC)\, e + Ew - LDz \rangle \\ &\quad = \sum_{i=1}^{2^{n_x}} \lambda_i\, \chi^T \begin{pmatrix} \mathcal{H}_i & PE & -PLD \\ * & 0 & 0 \\ * & * & 0 \end{pmatrix} \chi. \end{aligned} \tag{19}$$

We derive from (16)

$$\begin{aligned} &\langle \nabla V(e), (A - LC)\, e + Ew - LDz \rangle \\ &\quad \leq \sum_{i=1}^{2^{n_x}} \lambda_i\, \chi^T \begin{pmatrix} -\varepsilon I_{n_x} & 0 & 0 \\ * & \mu_w I_{n_w} & 0 \\ * & * & \mu_z I_{n_z} \end{pmatrix} \chi \\ &\quad = \chi^T \begin{pmatrix} -\varepsilon I_{n_x} & 0 & 0 \\ * & \mu_w I_{n_w} & 0 \\ * & * & \mu_z I_{n_z} \end{pmatrix} \chi \\ &\quad = -\varepsilon |e|^2 + \mu_w |w|^2 + \mu_z |z|^2. \end{aligned} \tag{20}$$

Note that solutions to (15) are defined for any initial condition, any positive time and any piecewise continuous inputs w and z in view of Assumption 5, according to Theorem 3.2 of **?**. In view of (20), for any $e_0 \in \mathbb{R}^{n_x}$, $w, z \in \mathcal{L}_2$, the corresponding solution of e to (15) verifies for any $t \geq 0$

$$\dot{V}(e(t)) \leq -\varepsilon |e(t)|^2 + \mu_w |w(t)|^2 + \mu_z |z(t)|^2, \tag{21}$$

from which we deduce that

$$\|e\|_{2,[0,t]} \leq \sqrt{\frac{\mu_w}{\varepsilon}} \|w\|_{2,[0,t)} + \sqrt{\frac{\mu_z}{\varepsilon}} \|z\|_{2,[0,t)} + \sqrt{\lambda_{\max}(P)} |e_0|, \tag{22}$$

which corresponds to (17) with $c = \sqrt{\lambda_{\max}(P)}$.

When $w = 0$ and $z = 0$, we immediately deduce that $e = 0$ is UGES for system (15) from (20). ■

Theorem 1 means that we can design L to ensure the exponential convergence of the state estimate to the true state, provided (16) holds. This matrix inequalities become linear after a standard change of variables, namely $W = PL$, we can also use (16) to minimize the $\mathcal{L}_2$-gains associated to the model disturbance w and the noise z, i.e. $\sqrt{\frac{\mu_w}{\varepsilon}}$ and $\sqrt{\frac{\mu_z}{\varepsilon}}$.

4. SIMULATIONS AND DISCUSSION

We have synthesized observer (12) for the electrochemical model described in Section 2 with the set of parameters given in Table A.1. This numerical resolution of the electrochemical model considers $N_{neg} = 4$ and $N_{pos} = 4$ samples with equivalent thickness. This is a good compromise between model accuracy and computation cost. The matrices A, B and K in equation (11) are given by

$$A = 10^{-2} \begin{pmatrix} -1.65 & -2.06 & -5.07 & -0.09 & -0.60 & -1.64 & -3.18 \\ 0.20 & -0.66 & 0.45 & 0 & 0 & 0 & 0 \\ 0 & 0.23 & -0.23 & 0 & 0 & 0 & 0 \\ 0 & 0 & 0 & -1.78 & 1.78 & 0 & 0 \\ 0 & 0 & 0 & 0.25 & -1.27 & 1.01 & 0 \\ 0 & 0 & 0 & 0 & 0.37 & -1.22 & 0.84 \\ 0 & 0 & 0 & 0 & 0 & 0.43 & -0.43 \end{pmatrix},$$

$$B = (0\,,\, 0\,,\, -0.5915\,,\, 0\,,\, 0\,,\, 0\,,\, 0.9424),$$

and

$$K = 10^3 (1.5372\,,\, 0\,,\, 0\,,\, 0\,,\, 0\,,\, 0\,,\, 0).$$

We then construct [1] C_i for $i \in \{1, 2, 3, 4\}$ from Assumption 5 considering the OCVs given Figure 2

$$\begin{cases} C_1 = (0\ 0\ 24.6186\ 0\ 0\ 0\ -639.0266) \\ C_2 = (0\ 0\ 24.6186\ 0\ 0\ 0\ -0.6460) \\ C_3 = (0\ 0\ 0.0583\ 0\ 0\ 0\ -639.0266) \\ C_4 = (0\ 0\ 0.0583\ 0\ 0\ 0\ -0.6460). \end{cases}$$

We have constructed the matrix L by solving inequality (16), which gives

$$\begin{aligned} L = (&-2.0264, -1.4581, 16.5015, \\ &-5.3127, 6.7625, -8.3333, -26.5529). \end{aligned}$$

To evaluate this observer, we have simulated it with an output signal not generated by model (9)-(10) but by an infinite-dimensional model solved by finite elements, see Section 2 of Raël and Hinaje (2013). The latter is more accurate than the electrochemical model described Section 2 (it notably does not rely on Assumption 1), and substitutes for the real battery data. The set of parameters used to run this model is also given in Table A.1. Notice that σ_e, the ionic conductivity, is constant and that σ_{D_e}, the ionic diffusion conductivity is set to zero in order to satisfy Assumption 2. To have a representative cycle, we have used a current profile derived from a referenced Plug-in Hybrid Electric Vehicles (PHEV) power profile given in Belt (2010) and we have repeated it seven times to test different depth of discharge. Figure (3), shows the convergence of the observer under this normalized PHEV profile. A white unbiased noise of $\pm 200\, mV$ has been added on the output of the infinite dimensional model to challenge the observer robustness. The first plot shows the current profile applied to the battery, the second plot shows the output h and its estimate, the third and fourth plots represent the surface lithium concentration of the negative and the positive electrode respectively and below them a zoom that shows what happens in the short time horizon. The other states are not represented for the sake of readability.

The simulation results given in Figure 3 clearly show the good speed of convergence and the robustness of the observer design and its robustness to noisy measurements.

[1] Recall that only four matrices C_i's are needed for the battery model, see the explanations after Assumption 5.

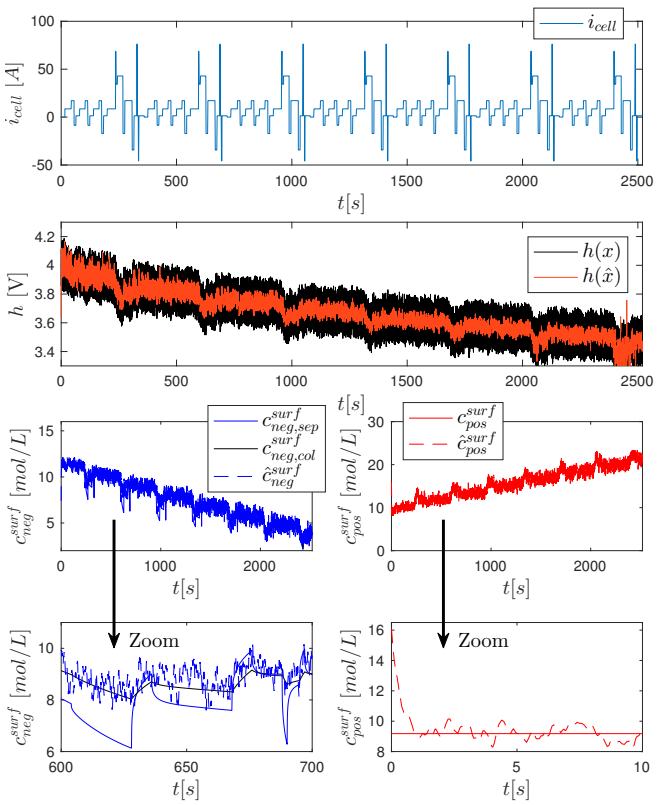

Fig. 3. Performance of the observer on a normalized PHEV current profile for a fully charged battery with estimated states initialized as if the battery was half discharged and under measurements noise.

Considering a huge initialization error, it takes about $2s$ for the estimates to reach a small neighbourhood of the corresponding states. It should be noticed here that the negative electrode is not homogeneous. Hence, the lithium concentrations near the separator and near the collector differ and two states representing the extreme case (one near the collector in black and one near the separator in blue) are given as reference. This simulation shows that the observer is more representative of what happens near the collector.

5. CONCLUSION

The presented observer shows promising results as shown in the simulation section and has a reasonable cost in terms of computation. Several applications can then come out as state of charge, health or function.

REFERENCES

Belt, J.R. (2010). Battery test manual for plug-in hybrid electric vehicles. Technical report, Idaho National Laboratory (INL).

Dey, S., Ayalew, B., and Pisu, P. (2015). Nonlinear robust observers for State-of-Charge estimation of Lithium-Ion cells based on a reduced electrochemical Model. *IEEE Transactions on Control Systems Technology*, 23(5), 1935–1942.

Di Domenico, D., Stephanopoulou, A., and Fiengo, G. (2010). Lithium-ion battery state of charge and critical surface charge estimation using an electrochemical model-based extended Kalman filter. *ASME J. Dyn. Syst. Meas. Control*, 1.

Doyle, M., Fuller, T.F., and Newman, J. (1993). Modeling of galvanostatic charge and discharge of the lithium/polymer/insertion cell. *Journal of the Electrochemical Society*, 140(6), 1526–1533.

Fan, X. and Arcak, M. (2003). Observer design for systems with multivariable monotone nonlinearities. *Systems & Control Letters*, 50(4), 319–330.

Johansson, A. and Medvedev, A. (2003). An observer for systems with nonlinear output map. *Automatica*, 39(5), 909–918.

Kong Soon, N., Chin-Sien, M., Yi-Ping, C., and Hsieh, Y.C. (2009). Enhanced coulomb counting method for estimating state-of-charge and state-of-health of lithium-ion batteries. *Applied Energy*, 86(9), 1506 – 1511.

Moura, S.J., Chaturvedi, N.A., and Krstić, M. (2012). PDE estimation techniques for advanced battery management systemsPart II: SOH identification. *American Control Conference (ACC)*, 566–571.

Plett, G.L. (2004). Extended Kalman filtering for battery management systems of LiPB-based HEV battery packs: Part 3. State and parameter estimation. *Journal of Power Sources*, 134(2), 277 – 292.

Prada, E., Di Domenico, D., Creff, Y., Bernard, J., Sauvant-Moynot, V., and Huet, F. (2013). A simplified electrochemical and thermal aging model of LiFePO4-graphite Li-ion batteries: Power and capacity fade simulations. *Journal of The Electrochemical Society*, 160(4), A616–A628.

Raël, S. and Hinaje, M. (2013). Using electrical analogy to describe mass and charge transport in lithium-ion batteries. *Journal of Power Sources*, 222, 112–122.

Saha, B., Goebel, K., Poll, S., and Christophersen, J. (2009). Prognostics methods for battery health monitoring using a bayesian framework. *IEEE Transactions on Instrumentation and Measurement*, 58(2), 291–296.

Santhanagopalan, S. and White, R.E. (2010). State of charge estimation using an unscented filter for high power lithium ion cells. *International Journal of Energy Research*, 34(2), 152–163.

Smith, K. and Wang, C.Y. (2006). Power and thermal characterization of a lithium-ion battery pack for hybrid-electric vehicles. *Journal of Power Sources*, 160(1), 662 – 673.

Urbain, M., Raël, S., Davat, B., and Desprez, P. (2007). State estimation of a lithium ion battery through kalman filter. In IEEE (ed.), *Power Electronics Specialists Conference*, 2804–2810.

Zemouche, A., Boutayeb, M., and Bara, G.I. (2008). Observers for a class of lipschitz systems with extension to h performance analysis. *Systems & Control Letters*, 57(1), 18–27.

Appendix A. PARAMETERS

Appendix B. DETAILED OUTPUT OF THE SYSTEM

For any $u \in \mathbb{R}$, the current-dependent component of the electrochemical model output mentioned in (10) $g(u)$ is

$$g(u) := g_1(u) + g_2(u) + g_3(u). \tag{B.1}$$

The term g_1 represents the activation overpotential of the positive electrode, g_2 is the activation overpotential of

Parameter [units]	**Negative electrode**	**Positive electrode**
Solid phase volume fraction ε [-]	0.332	0.330
Cell area $\mathcal{A}_{cell}$ $[m^2]$	1.0452	1.0452
Max. solid phase concentration c_s^{max} $[mol.L^{-1}]$	16.1	23.9
Thickness d $[\mu m]$	50	36
Lithium diffusion coef D $[m^2.s^{-1}]$	2×10^{-16}	3.6×10^{-16}
Electrolytic diffusion coef D_e $[m^2.s^{-1}]$	2.6×10^{-10}	2.6×10^{-10}
Exchange current density j_0 $[A.m^{-2}]$	36	26
Number of sample N [-]	4	4
Particle radius R $[\mu m]$	1	1
Electronic conductivity σ $[S.m^{-1}]$	100	10
Ionic conductivity σ_e $[S.m^{-1}]$	0.6329	0.6329
Ionic diffusion conductivity σ_{D_e} $[S.m^{-1}]$	0	0
Additional resistivity Ω_{add} $[\Omega]$	0	0

Table A.1. Physical parameters of the electrochemical model from Smith and Wang (2006)

Latin letters	
ε	Volume fraction [-]
σ	Conductivity $[S.m^{-1}]$
$\mathcal{A}$	Active surface $[m^2]$
a	Active surface per volume unit $[m^{-1}]$
c	Lithium concentration $[mol.m^{-3}]$
D	Lithium Diffusion coefficient $[m^2.s^{-1}]$
F	Faraday's constant $[C.mol^{-1}]$
N	Order of the model $[-]$
Q	Thermodynamic capacity $[A.h]$
R	Radius $[m]$
r	Radial coordinate $[m]$
$\mathcal{R}$	Gaz constant $[J.K^{-1}.mol^{-1}]$
S	Surface $[m^2]$
t	Time $[s]$
Subscript and superscript	
$cell$	Related to battery cell
col	Collector side
neg	Related to negative electrode
n_x	Size of vector x
pos	Related to positive electrode
s	Solid phase, stands for pos or neg
sep	Separator side
$surf$	Surface of an electrode

Table A.2. Symbol description

the negative electrode and g_3 are the electronic resistivity terms of the battery, they are defined as

$$
\begin{aligned}
g_1(u) &:= 2\frac{\mathcal{R}T}{F}\text{Argsh}\left(\frac{-R_{pos}}{6\,\varepsilon_{pos} j_0^{pos}\mathcal{A}_{cell}\,d_{pos}}u\right),\\
g_2(u) &:= -2\frac{\mathcal{R}T}{F}\text{Argsh}\left(\frac{R_{neg}}{6\,\varepsilon_{neg} j_0^{neg}\mathcal{A}_{cell}\,d_{neg}}u\right), \qquad \text{(B.2)}\\
g_3(u) &:= -\left(\frac{1}{2\,\mathcal{A}_{cell}}\left(\frac{d_{neg}}{\sigma_{neg}}+\frac{d_{pos}}{\sigma_{pos}}\right)+\Omega_{add}\right)u.
\end{aligned}
$$